Kinetically Driven Instabilities and Selectivities in Methane Oxidation

Young K. Park and Dionisios G. Vlachos
Dept. of Chemical Engineering, University of Massachusetts, Amherst, MA 01003

Ignitions, extinctions, and Hopf bifurcations in methane oxidation were studied as a function of pressure and inlet fuel composition. A continuous stirred-tank reactor was modeled with numerical bifurcation techniques, using the 177 reaction/31 species mechanism. Sensitivity and reaction pathway analyses were performed at turning points to identify the most important reactions and reactive species. Then, simulations were compared with experimental data. Multiple ignitions and extinctions as well as oscillations that are purely kinetically driven were found. Ignition to a partially ignited state with considerable reactivity of methane indicates possible narrow operation windows with high selectivities to partial oxidation products. At 0.1 atm, we found a selectivity of up to 80% to CO at 70% CH_4 conversion. The ignition to a fully ignited branch is associated with high selectivity to CO_2 and H_2O. The C2 chemistry inhibits the ignition of methane to the partially ignited branch. The methane ignition temperature exhibits two branches with respect to pressure, with only the low-pressure branch being dominant. Reaction path analysis at ignition conditions shows that the preferred pathway of CH_4 oxidation is to form CO and CO_2 through CH_2O and $CH_2(s)$ intermediates. However, at intermediate to high pressures, the recombination of CH_3 to C_2H_6 also becomes quite significant.

Introduction

Since the introduction of fire in prehistoric times, oxidation processes have become indispensable to our lives: from residential heating and internal combustion engines in cars, to oxidation reactors that produce many chemicals essential to daily life. Although oxidation processes are currently extensively implemented, these systems exhibit very complex nonlinear behavior that has not been well understood. Simple one-step global reactions with fitted rate constants are often inadequate to fully describe the wide range of species concentrations and bifurcation behavior that result at different reactor conditions (Coffee et al., 1983; Dryer, 1991). However, with the recent advances in computing technology and experimental techniques, there has been significant progress in developing detailed reaction mechanisms for oxidation of various fuels, especially for simple molecules such as hydrogen and methane (Warnatz, 1984; Miller and Bowman, 1989; Dagaut et al., 1991; Ranzi et al., 1994; Frenklach et al., 1995).

Correspondence concerning this article should be addressed to D. G. Vlachos.

Methane is the primary hydrocarbon species in natural gas. It is cheap and burns cleanly, making it an attractive alternative fuel for complete oxidation, and an important feedstock for partial oxidation to products such as synthesis gas (Hickman and Schmidt, 1993), formaldehyde, and methanol. Methane combustion reactors exhibit ignitions, extinctions, and multiple steady states, so understanding these phenomena is essential in order to identify regions of instability and to ensure safe operation during startup and shutdown of reactors.

Over the years, these have been numerous experiments on methane oxidation, primarily in shock tubes to evaluate induction times for ignition (Seery and Bowman, 1970; Spadaccini and Colkett, 1994), diffusion flames (Fotache et al., 1996), high-pressure partial-oxidation experiments to form methanol (Yarlagadda et al., 1988; Rytz and Baiker, 1991; Foulds et al., 1993), and catalytic oxidation (Griffin and Pfefferle, 1990; Williams et al., 1991; Behrendt et al., 1996; Veser and Schmidt, 1996). A few of these experiments, however, have addressed stationary ignition conditions of methane (Griffin

and Pfefferle, 1990; Williams et al., 1991; Behrendt et al., 1996; Fotache et al., 1996; Veser and Schmidt, 1996). On the other hand, theoretical studies on methane have focused on validating and improving proposed reaction mechanisms, predicting induction times, flame structures, and flame speeds (Williams, 1985; Smooke, 1991). There have been relatively few computational studies to better understand the bifurcation behavior of methane (Song et al., 1991; Vlachos et al., 1994). The work of Vlachos et al. first employed relatively detailed (46 reversible reactions) chemistry in stagnation flows to compute the bifurcation behavior of CH_4 (Vlachos et al., 1994). There is obviously a need to study the interplay of transport with complex chemistry in flow reactors in order to enhance performance of partial oxidation reactors while avoiding explosions.

A continuous stirred-tank reactor (CSTR) has been a prototype reactor for many years. In this reactor, the temperature and the concentrations are spatially homogeneous. Thus, modeling of a CSTR provides a limiting case for ignitions and extinctions in the absence of spatial gradients in temperature and concentrations. Furthermore, when an isothermal CSTR is modeled (as happens here), one can isolate pure-chemistry-driven (chain-branching) instabilities (Kalamatianos and Vlachos, 1995). By adding the energy balance, the effect of thermal feedback from chemical reactions on bifurcation can then be analyzed.

Kalamatianos and Vlachos have modeled and analyzed for the first time the stationary bifurcation behavior of hydrogen/air mixtures in a CSTR (Kalamatianos and Vlachos, 1995a,b). They found that for an isothermal CSTR, hydrogen exhibits a single ignition and extinction, and up to two Hopf bifurcations at high pressures. Our objective here is to extend the study of hydrogen/air oxidation to methane/air using detailed chemistry. One- and two-parameter continuation, sensitivity analysis, and reaction pathway analysis are performed to determine the effects of various parameters on the bifurcation behavior of the reactor.

Reactor Model and Detailed Chemistry

We model the homogeneous reaction of CH_4 with air in an isothermal CSTR. The species mass conservation equations in a CSTR are (Kalamatianos and Vlachos, 1995a):

$$\frac{dW_i}{dt} = -\frac{1}{\tau}(W_i - W_i^o) + \frac{1}{\rho} R_i M_i, \quad i = 1, \ldots, n, \tag{1}$$

where W_i is the mass fraction of species i, W_i^o is the mass fraction of species i at the inlet, M_i is the molecular weight of species i, R_i is the molar rate of production or consumption of species i, ρ is the mass density, τ is the residence time, and n is the number of species. The rate of production or consumption of species i is given by

$$R_i = \sum_{j=1}^{m} \nu_{ij} r_j, \tag{2}$$

where m is the number of gas-phase reactions, ν_{ij} is the stoichiometric coefficient of species i in the reaction j, and r_j is the rate of the jth reaction. The reaction rate constant is computed by the modified Arrhenius expression

$$k_j = A_j T^{\beta_j} \exp(-E_j/RT), \tag{3}$$

where k_j is the forward reaction rate constant of reaction j, A_j is the preexponential, β_j is the temperature exponent, E_j is the activation energy, T is the temperature, and R is the ideal-gas constant. The rate constants for reverse reactions are calculated from the rate constants of the forward reactions and their equilibrium constants.

Due to the importance of CH_4, several comprehensive mechanisms have been proposed (Miller and Bowman, 1989; Dagaut et al., 1991; Ranzi et al., 1994; Frenklach et al., 1995). Despite their complexity, some reaction steps are still under investigation. Here, the GRI-Mech 1.2 (Frenklach et al., 1995) is used to compute the gas-phase reaction rates. This reaction mechanism has been optimized for methane oxidation at lean-to-stoichiometric fuel mixtures, over a wide range of pressures and residence times, and represents one the most recent and comprehensive methane oxidation reaction mechanisms. The GRI's thermophysical data are used for equilibrium constant calculations. Some comparisons with the Miller–Bowman mechanism (Miller and Bowman, 1989) and the C1 subset of the GRI-Mech 1.2 to the full GRI-Mech 1.2 are also performed.

At steady state, Eqs. 1 are written in vector notation as

$$\boldsymbol{f}(\boldsymbol{u}, \lambda, \mu) = \boldsymbol{0}, \tag{4}$$

where λ and μ are two parameters of the system (called the primary and secondary bifurcation parameters), and $\boldsymbol{u}$ is the solution vector of mass fractions. The parameters that govern the state of the reactor include temperature, residence time, pressure, mixture composition, and heat effects, the latter depending on whether the reactor is isothermal or nonisothermal. The primary bifurcation parameter is chosen as the reactor temperature, while any parameter in Eqs. 1–3 can be considered as a secondary bifurcation parameter. Equations 4 are solved numerically using an arc-length continuation algorithm (Kalamatianos et al., 1997) and Newton's method.

After approximate ignition and extinction temperatures have been determined using the one-parameter continuation technique, a two-parameter continuation algorithm is used to determine the full range of bifurcation with respect to a secondary bifurcation parameter such as pressure, residence time, and equivalence ratio. At a turning point, the Jacobian $\boldsymbol{f}_{\boldsymbol{u}}$ of the system of Eqs. 4 is singular, and an eigenvalue of $\boldsymbol{f}_{\boldsymbol{u}}$ is zero. In addition to Eqs. 4, the following equations

$$\boldsymbol{f}_{\boldsymbol{u}} \boldsymbol{v} = \boldsymbol{0}, \tag{5a}$$

$$\boldsymbol{v}^T \boldsymbol{v} - 1 = 0 \tag{5b}$$

must be satisfied simultaneously, where $\boldsymbol{v}$ is the normalized eigenvector corresponding to the zero eigenvalue. So, for two-parameter continuation, the following extended system is solved

$$\boldsymbol{F}(\boldsymbol{U}(\mu), \mu) = \boldsymbol{0} \tag{6}$$

where $F=[f,\ f_v,\ v^Tv-1]^T$ and $U(\mu)=[u,\ \lambda,\ v]^T$. Superscript T denotes transpose. Details of the numerical algorithms are given elsewhere (Kalamatianos et al., 1997).

Effect of Reactor Temperature on Reactor Stability

In order to examine the effects of isothermal reactor temperature on ignitions and extinctions, we carry out one-parameter continuation simulations with respect to reactor temperature. Figure 1a shows the mole fraction of CH_4 in the reactor as a function of reactor temperature, for 0.02 atm, 1-ms residence time, and 9.5% inlet CH_4 in air. At low temperatures (below ~1,800 K), the mole fraction of CH_4 remains relatively unchanged with respect to temperature, and the system is on the extinguished branch. However, as the reactor temperature rises above 1,820 K, the outlet mole fraction of CH_4 decreases steadily. The branch between ~1,840 K and ~1,900 K is a *partially ignited branch*. At ~1,900 K, there is an ignition, characterized by a turning point. Further increase in temperature beyond the ignition point leads the system to a *fully ignited branch*, where most of the fuel is oxidized into CO, H_2, H_2O, and CO_2. Likewise, at high temperatures (above the ignition temperature), the system is on the ignited branch. As the temperature of the reactor is decreased along the fully ignited branch, a sudden change in CH_4 composition occurs at the extinction point where the system jumps to the partially ignited branch.

Although we term the turning points as ignition and extinction (a first set of turning points), we note that for CH_4, there is high reactivity prior to ignition and after extinction. This behavior is very different from the one of H_2, which shows almost no reactivity before ignition, and exhibits a very cuspy ignition turning point (Kalamatianos and Vlachos, 1995a).

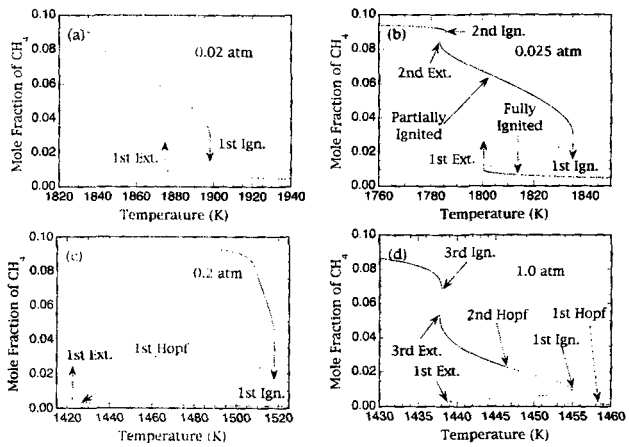

Figure 1. Mole fraction of CH_4 vs. temperature for reactor conditions of 10^{-3}-s residence time, 9.5% inlet CH_4 in air, and four different pressures indicated.

At low pressures, a single ignition and extinction exist (panel a). At a slightly higher pressure, a second pair of ignition and extinction emerges, indicating two ignited branches (panel b). At intermediate pressures, the second pair of ignition and extinction disappears, and a Hopf bifurcation point appears on the ignited branch (panel c). At a higher pressure, a third pair of ignition and extinction exists, and a second Hopf bifurcation point is found that has emerged from the first ignition turning point (panel d). Autocatalytic (isothermal) chemistry induces complex bifurcation behavior.

This high reactivity observed before ignition on the partially ignited branch suggests that even at low pressures such as 0.02 atm, the ignition may be influenced by thermal feedback in the case of nonisothermal reactors. The role of thermal feedback will be addressed in detail elsewhere (Park and Vlachos, 1997). Also, we should stress that the pool of radicals on the fully ignited and partially ignited branches are quite different. As a result, selectivities before and after ignition are expected to differ considerably.

Local stability analysis shows that the extinguished and ignited branches are stable steady states with respect to infinitesimally small perturbations. Between the ignition and the extinction points, a region of unstable steady states exists (indicated by the dashed line). In this regime, hysteresis is observed, and the solution of the system is determined by the reactor history. The convention of solid lines indicating stable branches and dashed lines indicating unstable branches is used throughout the rest of this article (except when clarity is necessary in complex figures).

The reactor model (Eqs. 1–3) is isothermal, and no thermal feedback from reaction exothermicity is taken into account. *To the best of our knowledge, this is the first time that isothermal autocatalytic chemistry (chain-branching) for CH_4/air mixtures is unambiguously shown to induce reactor hysteresis.*

Effect of Pressure on Reactor Stability

Figure 1a shows how temperature affects the CH_4 reactivity in an isothermal reactor for fixed reactor pressure, residence time, and inlet fuel composition. Next, we study the behavior of the system as a function of pressure. Panels b–d in Figure 1 show the effect of temperature on the reactor for various pressures. As the pressure of the system increases to 0.025 atm (Figure 1b), the first ignition and extinction are still present. However, at this pressure, a second pair of ignition and extinction also appears at a temperature of ~1,790 K. This second ignition occurs at the relatively high mole fraction of CH_4 and shows little reactivity before the turning point. Local stability analysis shows that the intermediate branch between the second ignition and extinction is unstable, whereas the intermediate branch between the second extinction and first ignition is stable (the partially ignited branch). This second set of turning points disappears at ~0.09 atm. The appearance of the second set of turning points better justifies our definition of a partially ignited branch we introduced earlier.

Figure 1c shows the mole fraction of CH_4 vs. reactor temperature at a higher pressure of 0.2 atm. At this pressure, the first ignition and extinction still persist, whereas the second set of ignition and extinction has indeed disappeared. There is also a Hopf bifurcation point on the fully ignited branch at ~1,426 K. This point appears from the first extinction point at around 0.055 atm [a Tokens Bogdanov (TB) point], and moves away from the turning point as the pressure increases.

A Hopf bifurcation point marks the beginning of an instability characterized by oscillations. For example, for these particular conditions, a decrease in temperature along the ignited branch below the Hopf point could lead to interesting situations. When the limit cycle surrounding the ignited branch is stable, we would see sustained oscillations. Extinc-

tion would then be oscillatory (Kalamatianos and Vlachos, 1995a,b). On the other hand, when the limit cycle is unstable, the system would jump to the extinguished branch. Extinction would then be determined from the Hopf point. Such behavior for H_2/air mixtures has been analyzed in detail by Kalamatianos and Vlachos (1995a).

Finally, Figure 1d shows the behavior of the system at a higher pressure of 1 atm. For these conditions, several interesting features are observed. First, a new set of turning points (third pair) has been formed at a lower temperature than the first set of turning points. The third set of turning points emerges at ~ 0.5 atm and disappears at ~ 1.05 atm. Second, there are two Hopf points. The second Hopf bifurcation point emerges at ~ 0.5 atm from the first ignition turning point, and shifts away from the turning point with increasing pressure. The first Hopf point is still found on the fully ignited branch, and continues to increase in temperature with increasing pressure. *This is the first time that we observe a Tokens Bogdanov point emerging from an ignition, that is, oscillations preceding ignition for a realistic chemistry system.* Third, the whole region between the two Hopf bifurcation points is unstable and physically, the reactor should exhibit sustained oscillations.

In order to confirm the existence of oscillations within the unstable regime, we can integrate Eqs. 1 with respect to time. An example is shown in Figure 2, which plots the mole fractions of CH_4 and CO_2 as a function of normalized time for the same conditions as in Figure 1d and a reactor temperature of 1,458 K. As expected, for both the fuel and an oxidation product, we see sustained oscillations that are periodic, with a period of about 10 residence times. The minimum CH_4 mole fraction corresponds almost to the maximum CO_2 mole fraction. The reactor shows relaxation-type oscillations for these conditions, spending more time in the unreactive state than in the reactive one. The amplitude of the oscillations is quite large, indicating that thermal effects would influence the oscillatory behavior.

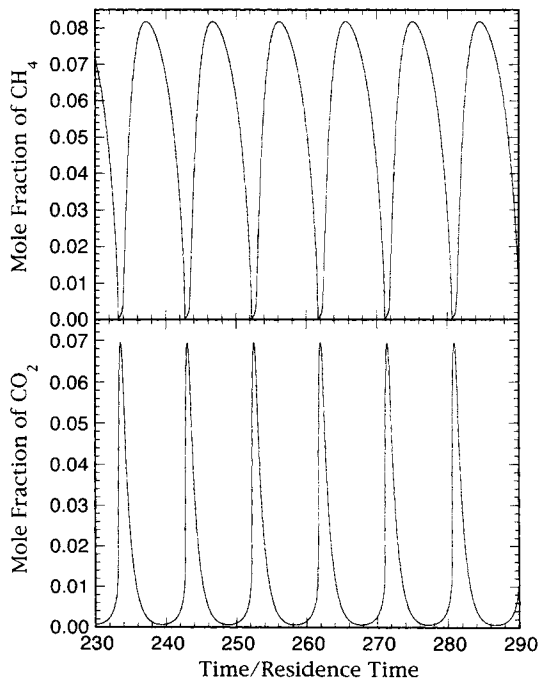

Figure 2. Mole fraction of CH_4 and CO_2 vs. normalized time for reactor conditions of 9.5% inlet CH_4, 10^{-3}-s residence time, 1 atm, and reactor temperature of 1,458 K, corresponding to the ignited branch in Figure 1d.

Both CH_4 (panel a) and CO_2 (panel b) show self-sustained relaxation-type oscillations.

Oscillations in hydrocarbon oxidation at low temperatures (~ 300–400 K) are well documented; they are known as cool flames (Dryer, 1991). *However, the oscillations found here for CH_4 oxidation at high temperatures have not been reported before.* Furthermore, results for different reaction mechanisms (discussed below) all exhibit Hopf bifurcation points on the fully ignited branches, indicating that oscillatory behavior for these conditions is a relatively robust feature of the reaction system. However, additional modeling and experiments are needed to further investigate the existence and the nature of these oscillations.

The panels in Figure 1 are several one-parameter bifurcation "cuts" that show the effect of pressure on bifurcation. A more systematic method to determine the range of multiplicity with respect to a secondary bifurcation parameter (e.g., pressure) is to use a two-parameter continuation algorithm, described by Eqs. 6 (see also Kalamatianos et al., 1997). Figure 3 is a two-parameter continuation plot, which shows the effect of pressure on ignition and extinction temperatures, for 9.5% inlet CH_4 in air. The ignition and extinction curves determine the regime of multiplicity, and merge at a higher and lower pressure, forming cusp points. Beyond the cusp points, there is reactivity, but no hysteresis.

The main ignition and extinction curve (first pair) span the entire pressure range, whereas the second and third set of ignitions and extinctions exist at low and high pressures, re-

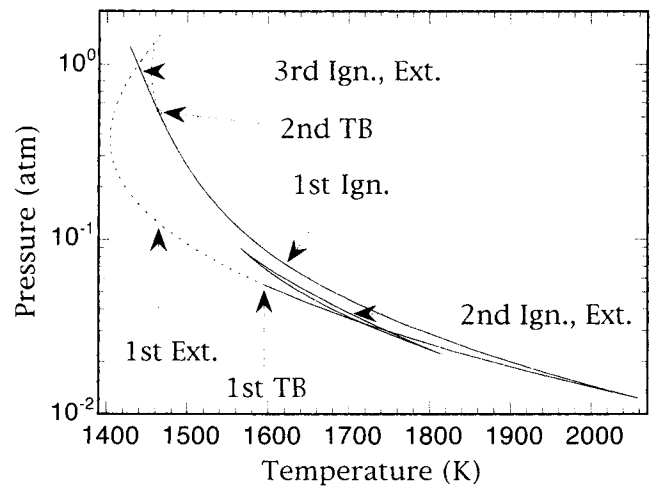

Figure 3. Two-parameter plot of pressure vs. ignition and extinction temperatures for reactor conditions of 9.5% inlet CH_4 in air and 10^{-3}-s residence time.

The squares indicate the initial pressure where a Hopf bifurcation emerges from a turning point (a Tokens Bogdanov point). An increase in pressure results in a decrease of ignition temperature. Three ignition–extinction loops are found. The main ignition exhibits two branches, with the second one being unstable.

spectively. The main ignition and extinction curves are depicted with a solid line at low pressures and a dashed line at intermediate to high pressures. Solid lines show turning points that connect a stable with an unstable branch (in one-parameter bifurcation diagrams such as the one shown in Figure 1), whereas dashed lines mark turning points that connect two unstable branches. The transition from dashed to solid lines occurs at the Tokens Bogdanov points where Hopf bifurcation points emerge from turning points. At pressures where an overlap exists between two sets of ignition and extinction curves (e.g., 0.05 atm or 0.8 atm), five multiple steady-state solutions exist.

Figure 3 shows that the main ignition temperatures exhibit two distinct branches. At low to moderate pressures, the ignition temperature decreases with increasing pressure (a first branch). At moderate pressures, the curve turns back on itself, and ignition temperatures increase with increasing pressure (a second branch). The same general trend is also seen for the extinction temperature. The second branch indicates an inhibition of ignition at moderate pressures by termination reactions that consume the radicals necessary to cause ignition. This turning-back behavior of the ignition curve is reminiscent of the H_2 case (Lewis and von Elbe, 1987; Kalamatianos and Vlachos, 1995a), where the depletion of H radicals through the reaction with O_2

$$H + O_2 + M \rightarrow HO_2 + M \qquad \text{(R33-R37)}$$

causes a strong inhibition effect at intermediate to high pressures. Even though this reaction is technically a propagation step, it competes with the chain-branching reaction

$$H + O_2 + M \rightarrow O + OH + M \qquad \text{(R38)}$$

and often inhibits H_2 flames because HO_2 is an inactive radical (Vlachos, 1995). This inhibition for H_2 is created by a third-order pressure dependence of the termination reaction as compared to a second-order pressure dependence of the main chain-branching mechanism. However, for CH_4, this inhibition (the second branch) continues only up to ~ 2 atm, and is unstable due to Hopf bifurcations. This suggests that unlike H_2, CH_4 does not have strong radical termination reactions that become dominant at high pressures. A sensitivity analysis discussed below confirms these ideas.

Although we consider the first ignition as the main ignition, we see from Figure 1 that the first ignition occurs at higher temperatures than the second or the third ignition. At conditions of multiple ignitions, the second or third ignition leads the system from an extinguished branch to a partially ignited branch, and the main ignition leads the system from a partially ignited branch to the fully ignited branch. Figure 4 shows the mole fraction of various species along the three ignition curves of Figure 3. Panel a shows that at the second or third ignition, the reactivity of CH_4 is relatively low, while at the first ignition, the reactivity of CH_4 is quite high, especially at high pressures. We have suggested earlier that the selectivities before and after ignition may differ considerably because the concentrations of active oxidizers OH and O are usually low before ignition. Panel b indicates that before the ignition to the partially ignited branch (low pressures), CH_2O

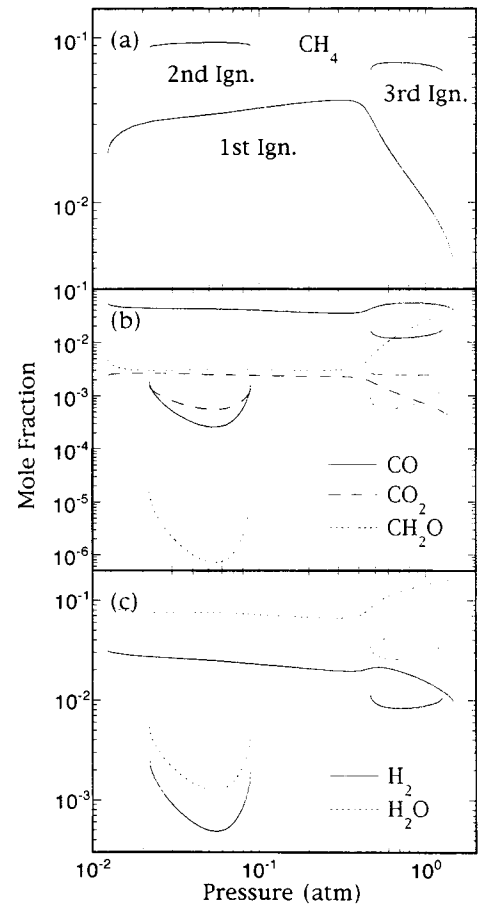

Figure 4. Various species mole fractions at ignition conditions corresponding to Figure 3.

At second and third ignition conditions, there is only slight reactivity of CH_4. However, at main ignition conditions, significant reactivity of CH_4 occurs, especially at high pressures. The selectivities to partial oxidation products are higher on the extinguished and partially ignited branches. For clarity, the convention of solid and dashed lines is not followed here.

and CO are preferred over CO_2 by more than two orders of magnitude. On the partially ignited branch, CH_2O oxidizes to CO due to higher concentrations of OH. As a result, CO is still preferred over CO_2, but the selectivity to CH_2O is reduced. At pressures above ~ 0.4 atm where high reactivity of CH_4 occurs, CO_2 becomes the most favorable carbon-containing product. Panel c shows the concentrations of hydrogen-containing products, namely H_2O and H_2. Similar to carbon-containing species, we see that the concentrations of H_2O and H_2 are higher at main ignition conditions, than prior to it. For these conditions, formation of H_2O is always preferred over H_2 for all pressures. These results indicate that *the temperature range between the onset of the partially ignited branch and the main ignition determines a possible favorable window of operation for partial oxidation products with moderate reactivity of CH_4.*

Effect of Inlet Fuel Concentration on Reactor Stability

Figure 5 shows the ignition and extinction temperatures as a function of the inlet mole fraction of CH_4 for two different

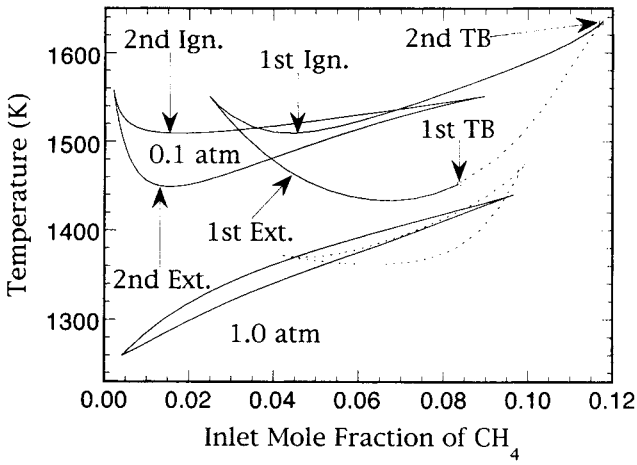

Figure 5. Two-parameter plot of ignition and extinction temperatures vs. inlet mole fraction of CH_4 for reactor conditions of 10^{-3}-s residence time and two different pressures of 0.1 atm and 1 atm.

Up to two ignition–extinction loops have been found. At low pressures, a minimum in ignition temperatures with composition occurs. At 1 atm, Hopf bifurcations appear at lower compositions as a pair before the turning points, causing the whole first ignition and extinction curves to be unstable at higher compositions.

pressures indicated. In general, all ignition and extinction temperatures are higher for lower pressures, in agreement with Figure 3. Two sets of ignitions and extinctions exist for both pressures, with the first set of turning points at fuel-rich conditions. Both the first ignition and extinction curves exhibit a shallow minimum at intermediate inlet fuel compositions, and the range of multiplicity increases as the pressure decreases. At low pressures, Hopf bifurcations occur both on the first ignition and extinction from Tokens Bogdanov points. As the pressure increases, these Hopf bifurcations shift to lower inlet CH_4 mole fractions. At 1.0 atm, the Hopf bifurcations have shifted to fuel lean conditions, and they emerge as a pair (a different bifurcation scenario). As the inlet mole fraction of CH_4 increases, these two Hopf bifurcations envelop the whole first ignition and extinction curves, causing them to be unstable.

Compared to the first ignition and extinction, the second ignition and extinction curves are qualitatively more affected by pressure. For example, at low pressures, both the second ignition and extinction curves show a minimum at very fuel-lean conditions. However, at a higher pressure of 1.0 atm, the second ignition and extinction temperatures decrease monotonically with decreasing inlet mole fraction of CH_4. Although pressure seems to have a strong effect on the qualitative behavior of the second ignition and extinction curves, it only weakly influences its range of multiplicity.

Figures 3 and 5 indicate that the multiple ignition/extinction loops are disconnected, at least for these conditions. We should note that additional isolated branches of turning points may exist. Besides the automatic two-parameter continuation simulations, we have also carried out many one-parameter cuts to examine for other possible multiplicities. We believe that the results shown in Figures 3 and 5 are probably complete ignition/extinction bifurcation diagrams.

After having presented the main features of bifurcation behavior, we first present below comparison with experiments. Then, chemistry interactions are analyzed for the bifurcation behavior presented earlier. In the analysis below, we focus primarily on the main ignition curves (first ignition).

Comparison with Experiments

Similar to Figure 3, the effect of pressure on the ignition limit of methane has also been studied in old batch experiments: a low-pressure study (Vanpée and Fally, 1952) and a high-pressure study (Townend and Chamberlain, 1936). Although these were batch experiments, their results show that for mixtures near the stoichiometric point of methane in air or in oxygen, increasing the pressure decreases monotonically the ignition or explosion temperature, which agrees qualitatively with our simulation results. Townend and Chamberlain's data also show that for batch reactors, ignition can occur at high pressures of above 7 atm. We believe that this extended ignition range, as compared to our results, is due to the thermal feedback in the batch reactor via the high reactivity of CH_4 prior to ignition (Park and Vlachos, 1997).

More recently, Law and coworkers have studied experimentally ignition of methane diffusion flames (Fotache et al., 1996). Again, this is quite a different reactor from a CSTR, where flow, multicomponent diffusion, and thermal feedback are all quite important. However, despite these differences, their results show that for a variety of CH_4 compositions and different strain rates, ignition temperatures decrease monotonically with increasing pressure. Ignition also occurs for their whole experimental pressure range of ~ 0.3 atm to ~ 10 atm. Recently, we have also obtained similar numerical results in premixed CH_4/O_2 flames near surfaces (Ziauddin et al., 1997). The experimental results agree qualitatively with our simulations here, and we believe that the differences between the experiments and our CSTR simulations (extended ignition range and turning-back behavior at intermediate pressures) are due to thermal effects (Park and Vlachos, 1997). Comparison of our CSTR simulations with experiments and simulations in very different reactor configurations indicates that *the CH_4 chemistry is primarily responsible for the shape of the pressure–temperature ignition curve.*

Very few experiments have been carried out to characterize ignition of CH_4 in a CSTR. Recently, Dagaut and coworkers have studied CSTR CH_4 oxidation at various residence times, pressures, and inlet CH_4 compositions (Dagaut et al., 1991; Tan et al., 1994). They measured the composition of various species as a function of reactor temperature using gas chromatography. In Figure 6, one set of their experimental results (1 atm, 0.1-s residence time, and 0.3% CH_4/6% O_2 in N_2) (Dagaut et al., 1991) is compared to our simulations. This particular set of data has been chosen because of the abrupt decrease in the CH_4 mole fraction as the temperature increases, indicating possible hysteresis that was not pursued further experimentally.

The bottom x-axis is the experimental reactor temperature, whereas the top x-axis is our simulated reactor temperature. Curves denote modeling and symbols denote experimental data for the various stable species. Figure 6 shows that our simulation predicts an ignition at around 1,025 K, whereas Dagaut's data show high reactivity at around 1,120 K.

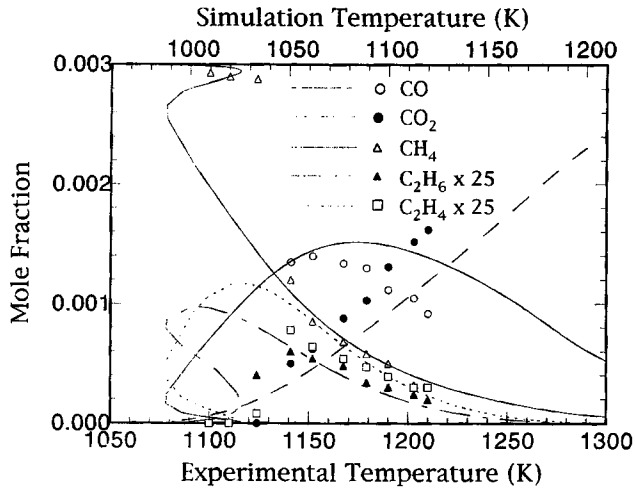

Figure 6. Comparison of our simulation to experimental data of Dagaut and coworkers (Dagaut et al., 1991).

Conditions are 1 atm, 0.1-s residence time, and 0.3% CH_4/6% O_2 in N_2. Symbols indicate experimental data and lines indicate simulation. The top x-axis shows the simulation temperature and the bottom x-axis shows the experimental temperature. Although simulations underpredict reactivity by ~90 K, the mole-fraction profiles of various species vs. temperature are in good agreement. For clarity, the convention of solid and dashed lines is not followed here.

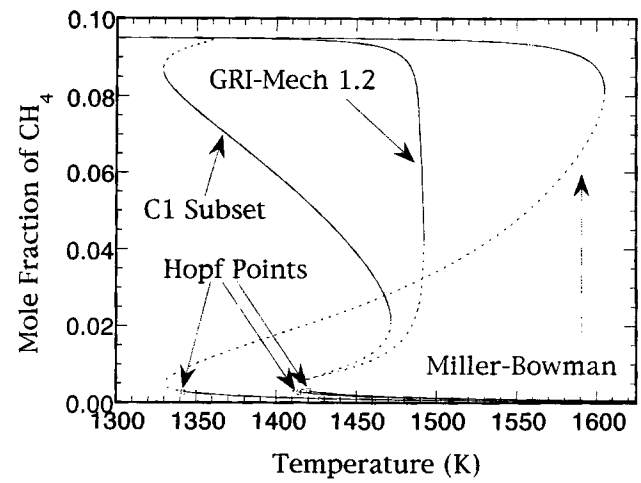

Figure 7. Mole fraction of CH_4 vs. reactor temperature for three reaction sets: the GRI-Mech 1.2, the C1 subset of the GRI-Mech 1.2, and the Miller–Bowman mechanism.

Conditions are 0.3 atm, 10^{-3}-s residence time, and 9.5% CH_4 in air. All three mechanisms exhibit a Hopf bifurcation point on the fully ignited branch, indicating that oscillations are a relatively robust feature of the methane oxidation chemistry. The C2 chemistry retards reactivity on the partially ignited branch.

This difference of ~90 K between simulations and Dagaut's experiments shown in Figure 6 represents about 10% relative error. Other comparisons at different reactor conditions (fuel lean and high pressures) show that the GRI-Mech 1.2 consistently underpredicts reactivity by 90 K to 150 K. This disagreement might be partly due to limitations of the GRI-Mech 1.2, which has been tested at temperatures greater than ~1,000 K, and partly to experimental difficulties, such as measurement of species concentrations and keeping the reactor well mixed and isothermal. However, despite this difference in temperature, the simulations predict species concentrations reasonably well, such as the maximum in CO concentration, the gradual increase in CO_2 concentration, as well as the concentrations of the C2 species. Upon ignition, both the simulation and experiments show good selectivities to C2 hydrocarbons and CO, which oxidizes further to CO_2 as the reactor temperature increases.

Comparison of Different Reaction Mechanisms

Over the years, many reaction mechanisms for homogeneous gas-phase methane combustion have been proposed, based on experiments and computational chemistry studies. We have chosen the 151 reaction/33 species Miller–Bowman mechanism (Miller and Bowman, 1989) to compare with the GRI-Mech 1.2 (Frenklach et al., 1995). Furthermore, to illustrate the importance of the C2 chemistry, a comparison between the full GRI chemistry and just the C1 chemistry of the GRI-Mech 1.2 mechanism was also considered.

Figure 7 shows a one-parameter plot using the three reaction sets, for conditions of 9.5% inlet CH_4, 1-ms residence time, and 0.3 atm. Compared to the GRI-Mech 1.2, the Miller–Bowman mechanism overpredicts ignition temperature by ~110 K (less than 10%). The shape of the unstable S-curve is also quite different. The Miller–Bowman mechanism predicts little reactivity before ignition, and the difference between ignition and extinction temperatures (hysteresis region) is large for these reactor conditions. In contrast, the full GRI-Mech 1.2 shows significant reactivity of CH_4 before ignition, and the difference between ignition and extinction temperatures (hysteresis region) is small.

The C1 chemistry also shows differences when compared to the full GRI-Mech 1.2. It predicts two pairs of ignitions and extinctions, a cuspy ignition with little reactivity, followed by a large stable region of reactivity (a partially ignited branch) and another ignition. The actual difference between the main ignition temperatures is only about 20 K, and the shape of the C1 chemistry S-curve is reminiscent of the GRI-Mech 1.2 mechanism at low pressures (see Figure 1b). Figure 7 indicates that the C2 chemistry may strongly retard ignition to the partially ignited branch. However, the unstable branch near the main extinction and the extinction of the fully ignited branch are only weakly affected by the C2 chemistry. Also, for all three reaction sets, Hopf bifurcation is predicted on the ignited branch, causing the extinction point on the ignited branch to be unstable. Again, although experiments are necessary to prove the existence of high-temperature oscillations, the prediction of Hopf bifurcation points by all three reaction sets indicate that oscillatory behavior is possibly real.

The main ignition and extinction curves for all three reaction sets are plotted as a function of pressure in Figure 8. The two-parameter bifurcation diagram shows that the Miller–Bowman mechanism predicts a much wider range of multiplicity compared to the GRI-Mech 1.2. In particular, multiplicity extends up to high pressures of ~40 atm. We believe that the GRI-Mech 1.2 should give a better represen-

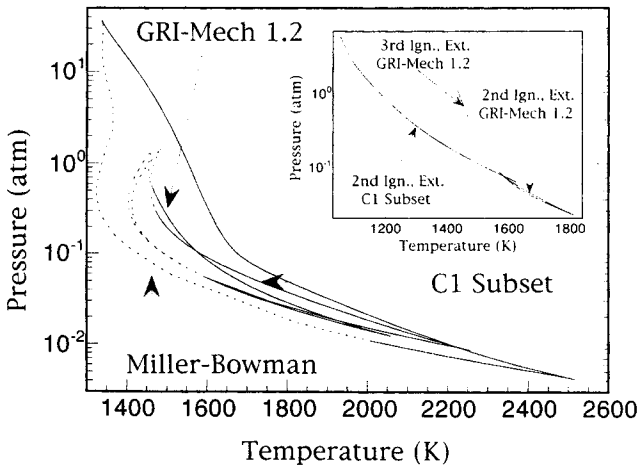

Figure 8. Two-parameter plot of pressure vs. main ignition and extinction temperatures for the three reaction sets: the GRI-Mech 1.2, the C1 subset, and the Miller–Bowman (MB) mechanism.

Conditions are 10^{-3}-s residence time and 9.5% CH_4 in air. The regime of multiplicity in terms of temperature and pressure is wider for the Miller–Bowman mechanism. The extinction temperature of the GRI-Mech 1.2 is slightly affected by the C2 chemistry. The insert shows the second and third ignition and extinction curves for the full GRI mechanism and the C1 subset. The C2 chemistry inhibits ignition at low reactivity.

tation of real systems. However, experiments are needed to clarify this issue.

Comparing the main ignition of the C1 chemistry to the full GRI mechanism, the C1 mechanism shows fairly good agreement with the GRI-Mech 1.2 at high pressures, but shows some deviations at intermediate and low pressures. Figure 8 indicates that the C2 chemistry slightly inhibits or slightly promotes the main ignition, depending on the pressure regime. Overall, however, the C2 chemistry does not much influence the main ignition (transition to a fully ignited branch) at high pressures. Extinction curves show very good agreement for almost the entire region of multiplicity, indicating that for any pressure, the first extinction pathways are only slightly influenced by the C2 chemistry.

All three reaction sets exhibit Hopf bifurcations on the extinction curve, starting from low (Miller–Bowman mechanism) and intermediate pressures (GRI mechanism), and continuing to high pressures. Only the C1 and GRI-Mech 1.2 mechanisms show Hopf bifurcations on the ignition curves, starting at moderately high pressures and continuing to high pressures. The C1 chemistry exhibits multiple ignitions and extinctions, whereas the Miller–Bowman mechanism shows only a single set of turning points for the reactor conditions considered. The insert in Figure 8 shows the multiple ignitions and extinctions (excluding the main pair) of the full GRI-Mech 1.2 and the C1 subset. Although the C2 chemistry does not have a significant influence on the main ignition and extinction, we see that it has a strong influence on the other pairs of ignition and extinction. Instead of two sets of ignition and extinction as shown for the GRI-Mech 1.2 chemistry, the C1 chemistry exhibits just one pair of secondary ignition and extinction curves that span a wide range of pressures. Also, at higher pressures (~ 1 atm), the second ignition temperature of the C1 chemistry is much lower than the third ignition temperature of the full GRI-Mech 1.2. This behavior indicates that *the C2 chemistry has a strong inhibiting effect on ignition at low reactivities*. This result is in agreement with Figure 7, which shows that the C1 chemistry induces a second ignition at low reactivities, whereas the full GRI chemistry exhibits only the main ignition.

It is generally believed that the difference of the C1 from the full GRI mechanism is most pronounced at fuel-rich conditions, because of the high concentration of fuel that can produce CH_3 radicals leading to various C2 hydrocarbons. Figure 9 shows a two-parameter continuation diagram of ignition and extinction temperatures vs. the inlet mole fraction of CH_4 for the C1 and the full GRI-Mech 1.2. The insert in Figure 9 is a clearer close-up of just the first ignition and extinction curves. The insert shows that the first ignition and extinction temperatures are only weakly affected by the inlet fuel composition (largest difference of ~ 25 K). However, for the C1 chemistry, the range of multiplicity is extended to fuel richer conditions. On the other hand, the second ignition and extinction curves are strongly inhibited by the C2 chemistry, by up to ~ 200 K. The differences in qualitative behavior of the curves, as well as the differences in ignition and extinction temperatures are quite large. Again, the results here are consistent with both Figures 7 and 8, where we see that the C2 chemistry inhibits ignition at low reactivities. In contrast to the general belief, Figure 9 also indicates that *the C2 chemistry affects considerably the ignition (transition) onto the partially ignited branch, even at fuel lean conditions*, due to CH_3 recombination leading to C_2H_4 and C_2H_5 (see reaction path analysis below).

Sensitivity Analysis at Ignition

The behavior of complex systems can often be better understood by examining the response of the system after perturbing one or more of its parameters. For a CSTR, such

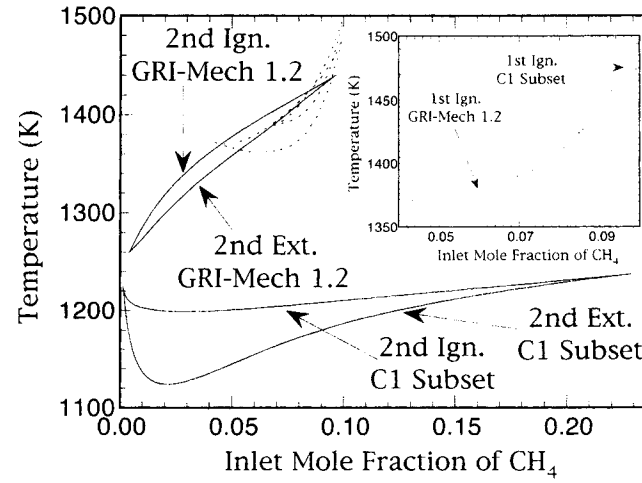

Figure 9. Two-parameter plot of ignition and extinction temperatures vs. inlet mole fraction of CH_4, for reactor conditions of 10^{-3}-s residence time and 1 atm.

The C2 chemistry only weakly influences the main ignition and extinction, but strongly affects secondary ignitions and extinctions (the transition to a partially ignited branch).

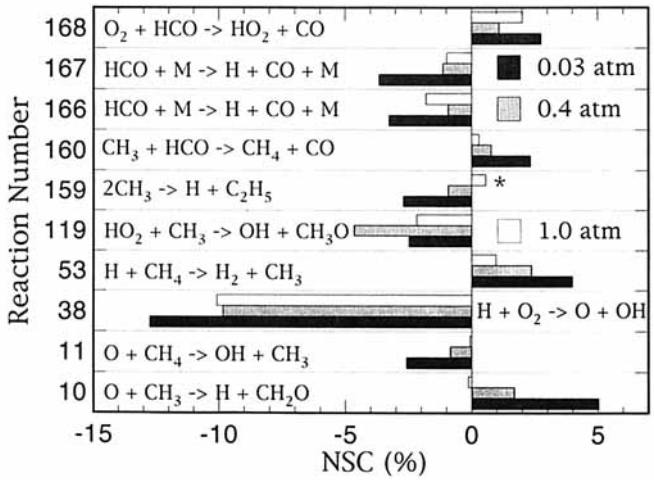

Figure 10. Sensitivity analysis of the GRI-Mech 1.2 (along the main ignition curve) at three different pressures indicated (cutoff threshold for NSC is ~ 2%).

All reactions proceed in the direction as written. Reaction with * denotes a negative rate (reverse reaction). The chain-branching reaction $H + O_2 + M \rightarrow OH + O + M$ is the primary promoting reaction. No strong inhibiting reactions exist for CH_4 oxidation, leading to an overall monotonic decrease in ignition temperature with increasing pressure (for most pressures shown in Figure 3).

parameters may be the reaction preexponentials, activation energies, inlet species concentrations, and mixing parameters. Here, we carried out sensitivity analysis (SA) along the main ignition curve, with respect to the reaction preexponentials, through a two-parameter continuation algorithm we introduced in detail elsewhere (Kalamatianos et al., 1997).

Figures 10 and 11 show the results for the GRI-Mech 1.2 and the C1 subset at three different pressures along the main ignition branches of the two-parameter pressure vs. ignition

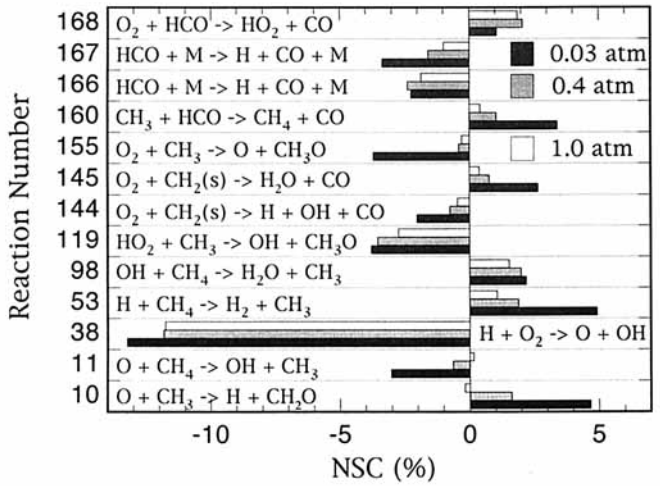

Figure 11. Sensitivity analysis of the C1 subset chemistry (along the main ignition curve) at three different pressures indicated (cutoff threshold for NSC is ~ 2%).

Most important reactions of the full mechanism are a subset of the important C1 chemistry, with all reactions showing the same trend in inhibiting or promoting.

temperature diagram shown in Figure 3. The normalized sensitivity coefficient (NSC) is defined as

$$\mathrm{NSC} = \frac{\partial \ln T_{ig}}{\partial \ln \mu} \times 100\% \tag{7}$$

where μ denotes the sensitivity analysis parameter. According to Eq. 7, a negative NSC means that the particular reaction promotes ignition. Likewise, a positive NSC denotes inhibition of ignition. Sensitivity analysis was carried out for all reactions, but only the reactions that had a significant influence on ignition temperatures are plotted in Figures 10 and 11.

For the GRI-Mech 1.2 (Figure 10), there are about ten reactions that strongly influence ignition. At low pressures, reactions seem to influence more strongly the ignition temperature. For all pressures, the most important reaction in promoting ignition is R38, the attack of molecular oxygen by radical H to form the radicals OH and O. This is a chain-branching reaction and is the only reaction that also strongly promotes the ignition temperature of H_2 flames for most conditions. Note that because CH_4 ignition temperatures are higher than those of H_2, the termination reaction R33–R37 is not as important as for H_2. Calculations show that the ratio of the rate of chain branching (R38) to the rate of termination (R33–R37) is always greater than 10 even for the lowest ignition temperatures that we have found for our conditions. The primary inhibition at low pressures is caused by R53, the reaction of H with CH_4 to form relatively unreactive H_2 and CH_3

$$H + CH_4 \rightarrow H_2 + CH_3. \tag{R53}$$

The decomposition of HCO through third-body collisions to CO and H (R166, R167) is a propagation reaction that forms the very reactive H radicals and promotes ignition. The competing reactions R160 and R168 deplete HCO (which could have been converted to H) to form stable molecules or relatively inert radicals. As a result, R160 and R168 inhibit ignition. The reaction of O with CH_4 to form OH and CH_3 (R11) is a chain-branching reaction forming OH, a primary species in the decomposition of CH_4. Thus, reaction R11 promotes ignition, especially at low pressures. R119, which also forms the active OH radical from relatively inert radicals, also promotes ignition.

The reaction of O with CH_3 to form H and CH_2O (R10) inhibits ignition at low pressures, because it reduces the number of radicals. The only important reaction that involves a C2 species is R159, the recombination of two CH_3 radicals to form H and C_2H_5, which is significant only at low pressures. The SA suggests that the C2 chemistry route is not very important in influencing ignition temperatures to the fully ignited branch (the main ignition) at these conditions. This is in agreement with the results shown in Figures 7–9. The CH_3 formed is primarily consumed to CH_2O and $CH_2(s)$. The path to CH_2O happens via O, a net termination reaction (R10). The consumption reactions of CH_3, R119, and R159, are relatively minor consumption paths as compared to the major path of R10.

At low pressures, when the C1 subset is used, ignition is sensitive to more reactions compared to the GRI-Mech 1.2. However, the set of important reactions contains all of the important reactions of GRI-Mech 1.2 (except R159). All of these reactions still show the same trends, that is, reactions that inhibit ignition for the GRI-Mech 1.2 also inhibit ignition for the C1 subset, and so forth. In particular, at low pressures, R155, the oxidation of CH_3 by O_2 to form O and CH_3O strongly promotes ignition, and R145, the oxidation of $CH_2(s)$ by O_2 to form H_2O and CO strongly inhibits ignition. However, at higher pressures, the reaction sets that influence ignition are almost identical for the C1 chemistry and GRI-Mech 1.2, indicating that we expect some deviations in ignition temperature at low pressures, but good agreement at higher pressures. This conclusion is consistent with the two-parameter pressure vs. ignition temperature diagram of Figure 8.

In contrast to both the C1 and the full GRI-Mech 1.2 mechanism, ignition in the Miller–Bowman mechanism is influenced only by a small number of reactions (sensitivity analysis not shown). R133, the attack of O_2 by H to form O and OH (R38 in GRI-Mech 1.2), is again important in promoting ignition, but is not the only dominant one. The thermal decomposition of C_2H_5 through third-body collisions to form H and C_2H_4 (R75), and the oxidation of CH_3 with O_2 to form CH_3O and O (R9) also considerably promote ignition. Only two reactions inhibit ignition: the reaction of CH_4 and H to form CH_3 and H_2 (R4) is again one of the dominant inhibiting reactions, as well as the net termination reaction of CH_3 with O to form CH_2O and H (R10). Similar to the GRI-Mech 1.2 and its C1 subset, all these reactions in the Miller–Bowman mechanism have a stronger influence at lower pressures.

In H_2/air mixtures, the termination reaction $H+O_2+M \rightarrow HO_2+M$ (R33–R37) has a third-order dependence on pressure that leads to strong inhibition of ignition at high pressures (Kalamatianos and Vlachos, 1995a; Vlachos, 1995). Consequently, a second branch forms over a wide pressure range where the ignition temperature increases as the pressure increases. In comparison to hydrogen, CH_4/air mixtures do not have termination reactions that are strongly influenced by pressure. According to the SA results in Figure 10, only R168 becomes more important at higher pressures, but is still only second-order pressure dependent. This termination reaction inhibits ignition just enough to cause a slight turning back of the ignition at higher pressures, but this phenomenon is very minor in comparison to hydrogen. To validate this hypothesis, we have omitted reaction R168 from the full mechanism and repeated the simulation shown in Figure 3. As expected, results show that the ignition temperature decreases monotonically with increasing pressure, with no turning-back behavior at higher pressures.

Reaction Pathway Analysis at Ignition

Sensitivity analysis has identified the reactions that affect ignition temperatures. However, to delineate further the bifurcation behavior, it is important to understand the primary reaction pathways through which important species are consumed and produced. We have already identified that radicals such as CH_3, HCO, H, OH, and O strongly influence ignition. Reaction pathway analysis (RPA) can give insight into how these radicals interact with other species, and what primary mechanisms create or destroy such radicals. RPA can be performed at any reactor conditions. Here, RPA was performed at different pressures along the main ignition curve of the GRI-Mech 1.2. In particular, by taking the solution vector of mass fraction (from a two-parameter continuation simulation) at a particular point such as an ignition, we can compute the relative contributions of all reactions to the formation and consumption of any species (Kalamatianos et al., 1997). The results for two different pressures are summarized in a reaction path diagram in Figure 12.

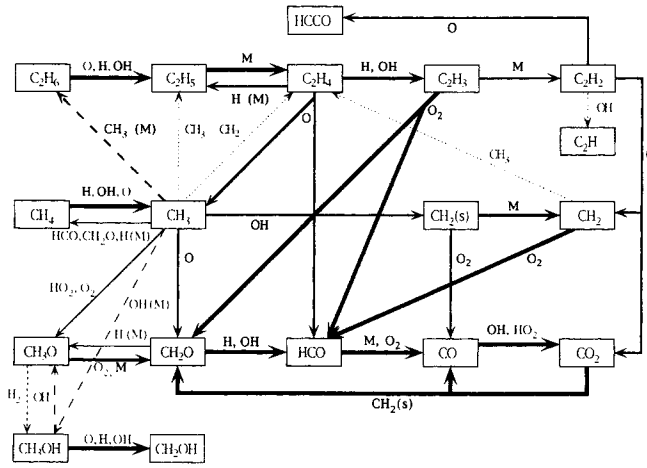

Figure 12. Reaction pathway diagram for two different pressures of 0.03 atm and 1 atm along the main ignition curve for the GRI-Mech 1.2.

Solid lines indicate dominant paths at all pressures, short dashes the dominant path at high pressure, and long dashes the dominant path at low pressures. The thickness of the lines indicates the importance of the consumption path of the species from where the arrow originates. Species over the lines denote reactants and bold type denotes species in the major pathways of destruction.

The results show that at low pressures (e.g., 0.03 atm), CH_4 reacts mainly with radical H and OH to form CH_3. About 10% of the CH_3 is consumed to form C_2H_5, which follows the C2 chemistry path as depicted in Figure 12. The majority of CH_3 reacts with O to form CH_2O, and with OH to form $CH_2(s)$. CH_2O reacts with H and OH to form HCO, whereas $CH_2(s)$ reforms to CH_2 through third-body collisions, which then oxidizes into HCO. HCO reacts with oxygen and thermally decomposes by third-body collisions to form CO, which can further oxidize to CO_2. So at low pressures, CH_2O, CH_2, and HCO are important intermediates of methane oxidation, and the C2 chemistry path is not very important for the transition to the fully ignited branch.

At high pressures, we see the same general trends with one main difference: at high pressures the route to C2 chemistry is primarily through the recombination of two CH_3 radicals to form C_2H_6, and about 25% of the total CH_3 consumption is through this pathway. So although the C1 pathway is still dominant at high pressures (e.g., 1 atm), the formation of C_2H_6 becomes significant as well. RPA analysis at intermediate pressures of around 0.4 atm indicates that the pathway to C_2H_6 from CH_3 becomes quite important, accounting for more than a third of the consumption of CH_3.

Interplay of Instabilities and Selectivities

In addition to predicting the range of multiplicity for different bifurcation parameters, we have also examined the effect of reactor conditions on selectivity. Partial oxidation products of methane, such as carbon monoxide, hydrogen, and methanol, are important reactants for the chemical industry, and identifying potential operating windows for their formation is an important task.

Figures 1 and 4 show that under certain conditions, there is significant reactivity of CH_4 before ignition to the fully ignited branch. Since the concentrations of oxidative radicals before ignition are low, one can expect that partial oxidation products could be preferred as also shown in Figure 4. The RPA at ignition shown in Figure 12 indicates that the preferred route of CH_4 oxidation is through CH_3 to form CO via the CH_2O and the $CH_2(s)$ pathways, implying that CH_2O and CO should be the major products in CH_4 oxidation for the conditions considered. Also, C2 hydrocarbons (e.g., C_2H_6) form at different conditions.

Figures 13 and 14 show the selectivity of various species and the conversion of CH_4 as a function of reactor temperature for two different reactor conditions. For carbon-containing species, selectivity is defined as the percentage of product that is formed from the total mass of carbon reacted from CH_4. For H_2 and H_2O, the same convention is used, using the total mass of hydrogen reacted from CH_4. Likewise, conversion of CH_4 is defined as the total mass of CH_4 reacted relative to the inlet.

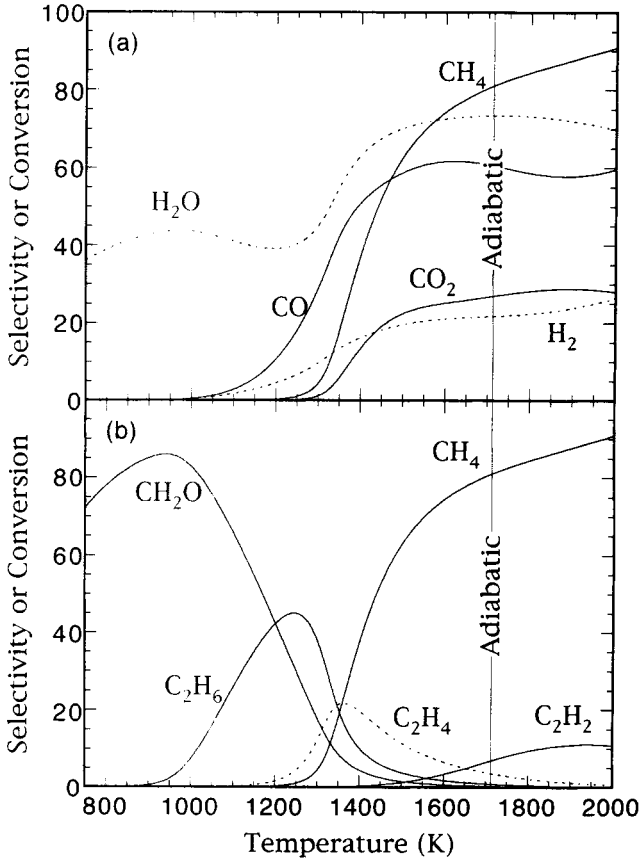

Figure 13. Selectivity of various major species as a function of reactor temperature for 15% inlet CH_4 in air, 10 atm, and 10^{-3}-s residence time.

The CH_4 line indicates conversion of CH_4. High selectivities to CH_2O and C_2H_6 are found before the onset of reactivity. Good selectivity to CO is found near the adiabatic temperature. For clarity, the convention of solid and dashed lines is not followed here.

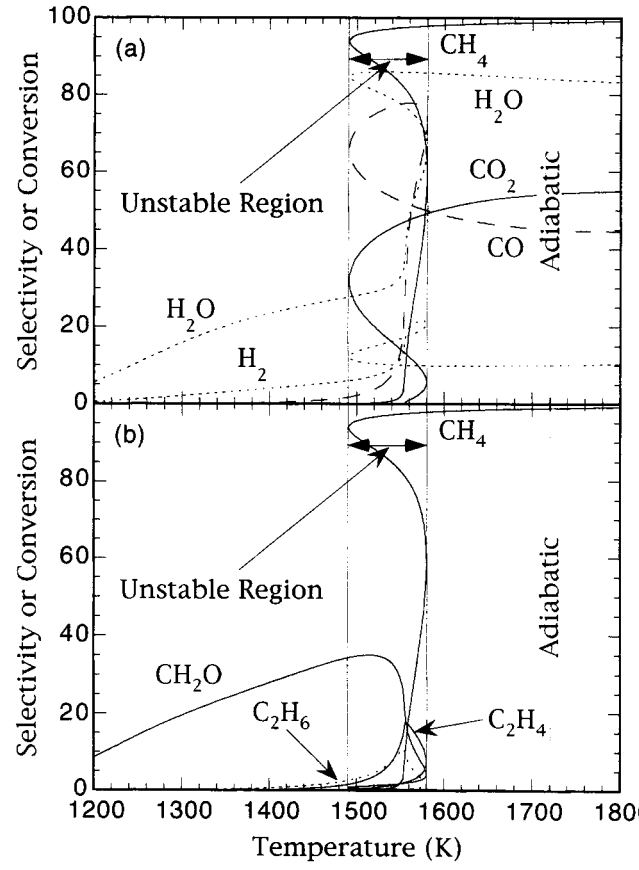

Figure 14. Selectivity of various species as a function of reactor temperature for 9.5% inlet CH_4 in air, 0.1 atm, and 10^{-3}-s residence time.

The unstable region indicates the temperature range enveloped by an ignition and extinction. Best selectivities to CO and H_2 are observed on the unstable branch. Quenching is necessary to obtain high selectivities to these products. For clarity, the convention of solid and dashed lines is not followed here.

The conversion of CH_4 and selectivity of various species shown in Figure 13 is for a reactor operating at 10 atm, 10^{-3}-s residence time, and 15% methane in air. Below ~1,200 K, the conversion of CH_4 is low, and the dominant carbon products are CH_2O and C_2H_6. This is consistent with our RPA, since CH_2O is a preferred intermediate species in CH_4 oxidation, and at high pressures, the recombination of CH_3 radicals to C_2H_6 is the preferred path toward the C2 chemistry. Above 1,300 K, significant conversion of CH_4 is seen, and the selectivity to CO increases rapidly to a maximum of ~60% at ~1,600 K. Since H_2 oxidizes faster than CO, the selectivity to H_2O is higher (~75%) at this temperature. Increasing the reactor temperature above ~1,600 K increases CH_4 conversion, but the selectivities of CO, CO_2, H_2, and H_2O remain relatively constant. The adiabatic operation temperature of ~1,716 K is also shown in Figure 13. For

these conditions, the best selectivities to CO and H_2 (without reactor heating) occur around or slightly below the adiabatic temperature.

When the reactor conditions are changed to a low pressure (0.1 atm) and to the stoichiometric mixture for complete oxidation (9.5% CH_4 in air) as shown in Figure 14, the system behaves quite differently. The temperature necessary for CH_4 reactivity is now quite high, above ~1,500 K. Below this temperature, CH_2O is the primary carbon species, while the selectivity to C_2H_6 is lower. Again, this is consistent with the RPA in Figure 12. There is an unstable region between the ignition and extinction points of ~1,580 K and ~1,490 K, respectively. The interesting feature within this unstable region is that there is a maximum selectivity to CO and H_2 of ~80% and 20%, respectively, with conversion of CH_4 greater than ~70%. We have observed such behavior of high selectivities within the multiplicity regime for many conditions. This behavior indicates that *the study of ignition and extinction may be important not only for safety concerns but also for selectivity aspects in chemical synthesis*. At the adiabatic operating temperature of ~1,720 K, formation of CO_2 and H_2O is favored over CO and H_2. This result indicates that at low pressures, reactor quenching is necessary to get good selectivities to CO and H_2.

The results in Figures 13 and 14 show two sets of quite different reactor conditions, where high selectivity to CO at high CH_4 conversion can be achieved. Although we did not search for optimal reactor conditions with best selectivities and conversion, other simulations were performed (not shown) to determine trends regarding selectivity. For example, for stoichiometric mixtures, increasing pressure increases selectivities to H_2O, CO_2, CH_2O, and C2 species, while decreasing selectivities to CO and H_2. The inlet composition of CH_4 has a large influence on selectivities. At 9.5% CH_4 in air, high selectivities to CO and H_2 are seen only at low pressures (not technologically interesting) on an unstable branch, such as the one shown in Figure 14. At fuel-rich mixtures, high selectivities to CO and H_2 are seen over a wide range of pressure, but reactor heating is often needed because mixtures may be outside the flammability regime. Selectivities to H_2 and C_2H_2 are the most sensitive to inlet CH_4 concentration, increasing with increasing CH_4 concentration. At conditions where the system can operate adiabatically, the best selectivities to CO and H_2 are seen below the adiabatic operation temperature, indicating that for gas-phase partial oxidation of CH_4, reactor quenching improves selectivities.

Conclusions

Using the GRI-Mech 1.2, the bifurcation behavior of homogeneous combustion of CH_4 in air has been simulated for the first time in a CSTR. Comparison with experiments shows that the GRI-Mech 1.2 gives qualitative agreement with data in other reactors, and semiquantitative agreement with data in a CSTR. Results show multiple ignitions, extinctions, and oscillations for various pressures and inlet CH_4 compositions, and up to five multiple steady states. Up to two Hopf bifurcations have been found. A Hopf bifurcation that emerges from an ignition point has been observed for the first time for realistic chemistry systems, implying oscillations prior to ignition. These instabilities stem purely from isothermal chemistry, which involves autocatalytic chain-branching steps.

Comparison with the Miller–Bowman mechanism shows that the GRI-Mech 1.2 predicts a smaller range of bifurcation with respect to pressure, and predicts lower ignition and higher extinction temperatures. Analysis of the C1 subset of the full mechanism shows that the C2 chemistry is not very important for the main ignition (transition to the fully ignited branch) and extinction for the conditions studied. However, the C2 chemistry inhibits considerably the transition to a partially ignited state, both as a function of pressure and inlet fuel composition. Sensitivity analysis at ignition shows that the primary promoting reaction for ignition is the radical chain-branching reaction, R38, which forms O and OH radicals. Inhibition occurs primarily through the depletion of H and O radicals by reactions R53 and R10 and loss of HCO to inert species (reactions R168 and R160). However, unlike hydrogen/air mixtures, there is no inhibition reaction that is strongly influenced by pressure. Only R168 becomes slightly dominant at higher pressures, producing a turning-back effect of the pressure–ignition curve diagram. Reaction pathway analysis shows that the primary route of CH_4 oxidation is the decomposition to CH_3 followed by the CH_2(s) and CH_2O pathways to CO. At intermediate to high pressures, recombination of CH_3 to C_2H_6 becomes a significant pathway to the C2 chemistry.

High selectivity to CH_2O and C_2H_6 is found at low CH_4 conversions and high pressures. On the other hand, high conversion of CH_4 to CO and H_2 occurs at low pressures (not technologically interesting) or fuel-rich mixtures. When multiple ignitions exist, the ignition to a partial ignited branch often indicates the onset of conditions where best selectivities to partial oxidation products can be achieved. In particular, the temperature window for chemical synthesis is near or between the second or third ignition (transition to partially ignited state) and the first ignition (transition to the fully ignited state), but is relatively narrow. High selectivities to CO and H_2 may occur within unstable branches between ignition and extinction, and upon ignition, reactor quenching may be essential to obtain good selectivity. This result also indicates that the study of the bifurcation behavior of such systems is necessary not only for safety aspects, but also to better understand the mechanisms that control formation of partial oxidation products.

Acknowledgment

The authors thank the Office of Naval Research, with Dr. G. D. Roy through a Young Investigator Award, under Contract N00014-96-1-0786, and the donors of The Petroleum Research Fund, administered by the American Chemical Society, for partial support of this research. One of the authors (Y. K. P.) is an American Chemical Society-Petroleum Research Fund Fellow.

Literature Cited

Behrendt, F., O. Deutschmann, R. Schmidt, and J. Warnatz, "Investigation of Ignition and Extinction of Hydrogen-Air and Methane-Air Mixtures Over Platinum and Palladium," *Proc. Symp. in Catalysis, Heterogeneous Hydrocarbon Oxidation*, ACS Meeting, New Orleans, LA, p. 48 (1996).

Coffee, T. P., A. J. Kotlar, and M. S. Miller, "The Overall Reaction Concept in Premixed, Laminar, Steady State Flames. I Stoichiometries," *Combust. Flame*, **54**, 155 (1983).

Dagaut, P., J. Boettner, and M. Cathonnet, "Methane Oxidation: Experimental and Kinetic Modeling Study," *Combust. Sci. Tech.*, **77**, 127 (1991).

Dryer, F. L., "The Phenomenology of Modeling Combustion Chemistry," *Fossil Fuel Combustion*, W. Bartok and A. F. Sarofim, eds., Wiley, New York, p. 121 (1991).

Fotache, C. G., T. G. Kreutz, and C. K. Law, "Ignition of Counterflowing Methane versus Heated Air under Reduced and Elevated Pressures," *Combust. Flame* **108**, 442 (1997).

Foulds, G. A., B. F. Gray, S. A. Miller, and G. S. Walker, "Homogeneous Gas-phase Oxidation of Methane Using Oxygen as Oxidant in an Annular Reactor," *Ind. Eng. Chem. Res.*, **32**, 780 (1993).

Frenklach, M., H. Wang, M. Goldenberg, G. P. Smith, D. M. Golden, C. T. Bowman, R. K. Hanson, W. C. Gardiner, and V. Lissianski, *GRI-Mech — An Optimized Detailed Chemical Reaction Mechanism for Methane Combustion*, Gas Research Institute, Rep. No. GRI-95/0058 (1995).

Griffin, T. A., and L. D. Pfefferle, "Gas Phase and Catalytic Ignition of Methane and Ethane in Air Over Platinum," *AIChE J.*, **36**, 861 (1990).

Hickman, D. A., and L. D. Schmidt, "Production of Synthesis Gas by Direct Catalytic Oxidation of Methane," *Science*, **259**, 343 (1993).

Kalamatianos, S., Y. K. Park, and D. G. Vlachos, "Two-parameter Continuation Algorithms for Computing Ignitions and Extinctions: Sensitivity Analysis, Parametric Dependences, Mechanism Reduction, and Stability Criteria," *Combust. Flame* (1997).

Kalamatianos, S., and D. G. Vlachos, "Bifurcation Behavior of Premixed Hydrogen/Air Mixtures in a Continuous Stirred Tank Reactor," *Combust. Sci. Tech.*, **109**(1–6), 347 (1995a).

Kalamatianos, S., and D. G. Vlachos, "Dynamics Near Ignitions and Extinctions of Premixed H_2/Air Mixtures," Eastern States Section, *Chemical and Physical Processes in Combustion*, The Combustion Institute, Worcester, p. 131 (1995b).

Lewis, B., and C. von Elbe, *Combustion, Flames and Explosions of Gases*, 3rd ed., Academic Press, Orlando, FL (1987).

Miller, J. A., and C. T. Bowman, "Mechanism and Modeling of Nitrogen Chemistry in Combustion," *Prog. Energy Combust. Sci.*, **15**, 287 (1989).

Park, Y. K., and D. G. Vlachos, "Isothermal Chain-branching, Reaction Exothermicity, and Transport Interactions in the Stability of Methane/Air Mixtures," *Combust. Flame* (1997).

Ranzi, E., A. Sogaro, P. Gaffuri, G. Pennati, and T. Faravelli, "A Wide Range Modeling Study of Methane Oxidation," *Combust. Sci. Technol.*, **96**, 279 (1994).

Rytz, D. W., and A. Baiker, "Partial Oxidation of Methane to Methanol in a Flow Reactor at Elevated Pressure," *Ind. Eng. Chem. Res.*, **30**, 2287 (1991).

Seery, D. J., and C. T. Bowman, "An Experimental and Analytical Study of Methane Oxidation Behind Shock Waves," *Combust. Flame*, **14**, 37 (1970).

Smooke, M. D., ed., *Reduced Kinetic Mechanisms and Asymptotic Approximations for Methane-Air Flames*, Springer-Verlag, Berlin (1991).

Song, X, W. R. Williams, L. D. Schmidt, and R. Aris, "Bifurcation Behavior in Homogeneous-Heterogeneous Combustion: II. Computations for Stagnation-Point Flow," *Combust. Flame*, **84**, 292 (1991).

Spadaccini, L. J., and M. B. I. Colkett, "Ignition Delay Characteristics of Methane Fuels," *Prog. Energy Combust. Sci.*, **20**, 431 (1994).

Tan, Y., P. Dagaut, M. Cathonnet, and J. C. Boettner, "Natural Gas and Blends Oxidation and Ignition: Experiments and Modeling," *Proc. Symp. on Combustion*, The Combustion Institute, Pittsburgh, p. 1563 (1994).

Townend, D. T. A., and E. A. C. Chamberlain, "The Influence of Pressure on the Spontaneous Ignition of Inflammable Gas-Air Mixtures IV—Methane-, Ethane-, and Propane-Air Mixtures," *Proc. Roy. Soc. (London)*, **A154**, 95 (1936).

Vanpée, M., and G. Fally, "La Limite Supérieure d'Inflammation des Mélanges de Méthane et d'Oxygène," *Bull. Soc. Chim. Belg.*, **61**, 474 (1952).

Vesser, G., and L. D. Schmidt, "Ignition and Extinction in the Catalytic Oxidation of Hydrocarbons over Platinum," *AIChE J.*, **42**, 1077 (1996).

Vlachos, D. G., "The Interplay of Transport, Kinetics, and Thermal Interactions in the Stability of Premixed Hydrogen/Air Flames Near Surfaces," *Combust. Flame*, **103**, 59 (1995).

Vlachos, D. G., L. D. Schmidt, and R. Aris, "Ignition and Extinction of Flames Near Surfaces: Combustion of CH_4 in Air," *AIChE J.*, **40**(6), 1005 (1994).

Warnatz, J., "Rate Coefficients in the C/H/O System," *Combustion Chemistry*, W. C. Gardiner, Jr., ed., Springer-Verlag, Berlin, p. 197 (1984).

Williams, F. A., *Combustion Theory: The Fundamental Theory of Chemically Reacting Flow Systems*, Benjamin/Cummings, Menlo Park, CA (1985).

Williams, W. R., M. T. Stenzel, X. Song, and L. D. Schmidt, "Bifurcation Behavior in Homogeneous-Heterogeneous Combustion: I. Experimental Results Over Platinum," *Combust. Flame*, **84**, 277 (1991).

Yarlagadda, P. S., L. A. Morton, N. R. Hunter, and H. D. Gesser, "Direct Conversion of Methane to Methanol in a Flow Reactor," *Ind. Eng. Chem. Res.*, **27**, 252 (1988).

Ziauddin, M., A. Balakrishna, D. G. Vlachos, and L. D. Schmidt, "Ignition of Methane Flames in Oxygen Near Inert Surfaces: Effects of Composition, Pressure, Preheat and Residence Time," *Combust. Flame* (1997).

Manuscript received Jan. 9, 1997, and revision received Apr. 14, 1997.